Vibrational Analysis of Molecular Interactions in Aqueous Glucose Solutions. Temperature and Concentration Effects

Maria Elena Gallina, Paola Sassi,* Marco Paolantoni, Assunta Morresi, and Rosario Sergio Cataliotti†

Dipartimento di Chimica, Università di Perugia, Via Elce di Sotto, 8, 06100 Perugia, Italy, and Istituto Nazionale di Fisica della Materia, Sezione di Catania, 95100 Catania, Italy

Received: October 28, 2005; In Final Form: March 7, 2006

A vibrational analysis using FTIR and Raman spectroscopies was carried out on aqueous glucose solutions with a wide range of solute molar fractions and temperatures. The analysis was aimed at revealing structural changes in the local hydrogen-bonding (HB) network of liquid water, correlating these with the conservative properties of biomolecules, and comparing them with those of other sugars. The results of our measurements clearly show that the action of glucose is 2-fold; on one hand, there is a linkage with free hydroxyls of water; on the other, there is a slight lessening of the ordered (tetrahedral) H-bonded assembly of bulk H_2O. These opposite effects do not balance each other, so the average HB interaction strength decreases on increasing glucose concentration. As a result, there is a reduction in the temperature dependence of solutions structure. In our opinion, this could be related to the low bioprotective action of this carbohydrate.

1. Introduction

It has been known for about half a century that, under severe drying and cooling conditions, sugar aqueous solutions have bioprotective and conservative effects on the biological polymers present in foods and drugs. Such effects have been ascertained both for solutions of simple monosaccharides such as glucose and fructose and for those of disaccharides as well as polysaccharides such as dextran.[1−3] These conservative properties are also found in some plants and spores; they produce large amounts of trehalose under dry and/or thermal shock. Thanks to this sugar production, these organisms can survive for many years in an anhydrobiotic state and retrieve all of their functions when rehydrated.[4] While technological and industrial applications of these bioprotective properties are widely employed today in the long-time storage of foods and drugs,[5] there is no univocal interpretation of the interaction mechanisms that give origin to these effects. The involvement of hydrogen bonding (HB) interactions is considered of primary importance, and a large amount of research is therefore still carried out in this field, both through theoretical calculations and model designs and by adopting various experimental approaches. Aqueous solutions of carbohydrates are widely studied inasmuch as they constitute useful models for understanding more complex biological systems. Water hydroxyls play a competitive role with the sites of carbohydrates for intra- and intermolecular HB formation; this competition influences their conformational flexibility with an entropy cost largely compensated for by the formation of new hydrogen bonds.[6−11]

As far as the conservative properties of sugar aqueous solutions are concerned, among the many hypotheses formulated there are two that still prevail in this research field. In the first,[12] the preservative mechanism is attributed to the partial replacement of water by the carbohydrate molecules in the HB network sites; this would produce a sort of encapsulation of the biological compounds, so that sugars would develop their protective effects by acting as water replacers. Molecular dynamics simulations strongly support this thesis, especially in the case of glucose solutions.[13−17]

A different hypothesis is suggested by the results of various vibrational spectroscopic, dielectric, X-ray, and neutron diffraction techniques.[18−26] The authors of these studies assert that carbohydrates, especially disaccharides such as trehalose and sucrose, act as destructuring agents for the long-range tetrahedral HB network of bulk water. Especially at higher concentrations, they impede the easy formation of ordered regions. In other words, the protective and conservative action of these disaccharides toward biological compounds consists of drastically reducing the so-called *icelike* water in their solutions, i.e., highly ordered water structure for which the arrangement is similar to that of the crystalline state.

There is no doubt that the high concentration aqueous solutions of carbohydrates present high viscosity values and high glass transition temperatures.[27] Glassy matrixes confer stability on labile products, causing the kinetic arrest of physical properties such as translational and rotational diffusion and of chemical processes such as reactions contributing to product degradation.[5] It has been reported[17,28] that when sugar concentration increases, the T_{Glass} increases as well, and glass can be obtained more easily, even close to room temperature. Sugars thus modify the HB network of bulk water considerably, producing a long-range disordered structure not arranged to freeze easily. In this context, trehalose has been found to have the highest T_{Glass} and the highest protective character toward biopolymers among a series of carbohydrates.[29] Magazù and co-workers[18−26] also demonstrated that this sugar has stronger power in destructuring the ordered assemblies of water.

As regards the ordered structure of water, the common reference is described in terms of a dynamic three-dimensional network of hydrogen bonds, established between H-donor OH groups of one molecule and H-acceptor lone pairs of other molecules. Extended in space, this is the so-called "open

* Corresponding author. E-mail: sassipa@unipg.it.
† Istituto Nazionale di Fisica della Materia.

10.1021/jp056213y CCC: $33.50
Published on Web 04/07/2006

structure", which is characteristic of hexagonal ice I_h. In liquid water, besides this icelike structure, large amounts of "closed structures", i.e., regions of defective hydrogen bonds, are present together with the open ones.[30] Since the local arrangement of hydrogen bonds is continuously broken and reformed at a picosecond time scale, both open and closed structures can be observed by using probes with shorter characteristic time scales. Vibrational spectroscopy at the OH-stretching frequencies is a useful probe for such an analysis, as the observation time is on the order of hundredths of a picosecond.

In our laboratory, HB interactions were investigated in liquid alcohols[31−35] and in alcohol/water mixtures[36] using IR and various scattering spectroscopies. We now wish to extend this study to aqueous solutions of sugars. Although there are no remarkable differences between the aqueous solutions of glucose and its dimer trehalose in relation to certain macroscopic properties such as solubility, density, viscosity, etc., trehalose has been shown to be the most active sugar in the bioprotective and conservative action of biopolymers. The aim of this paper is to establish the amount and strength of the hydrogen bond interactions in the aqueous solutions of glucose. In other words, we intend to learn how much glucose influences the modification of bulk water structure, in comparison with the strong action already observed for trehalose. To this end, we have used vibrational spectroscopic tools including IR and Raman spectra in the OH-stretching region. Moreover, temperature and concentration effects have been detected and are discussed here as well.

2. Experimental Section

(a) Chemicals. D-(+)-Glucose was obtained from Fluka Sigma-Aldrich with purity greater than 99.5%. It was dissolved in pure water, obtaining solutions whose concentrations varied from 0.029 to 0.12 mole fraction (hereafter indicated as x_G). All solutions were freshly prepared and conditioned for ca. 1 h before the measurements, to allow the anomeric equilibrium to be established.

Doubly distilled and deionized water was prepared in our laboratory and its purity was tested through spectroscopic methods in comparison with literature data. To avoid scattering from dust particles, the solutions were purified through a Millipore filter.

Amorphous sugar was prepared by melting crystalline α-D-glucose in a glass ampule with subsequent quench cooling. The melting was performed under nitrogen-saturated atmosphere, maintaining the temperature at 160 °C for 20 min.

(b) Spectra. Infrared spectra of water and glucose solutions were measured using a FTIR model IFS113V Bruker spectrometer with a resolution of 1 cm^{-1} in the spectral region between 370 and 5000 cm^{-1}. The measurements were executed at temperatures ranging from 5 to 80 °C, with a sample-chamber pressure of ca. 3 mbar to avoid air humidity interference. A cell with KRS5 windows was used, thus giving a high signal/noise ratio in the entire MIR range.

Raman spectra were recorded using an ISA Jobin-Yvon model U1000 double monochromator having 1 m focal length holographic gratings and photon counting detection. The exciting source was a Coherent model Innova 90 argon ion laser used in single-line excitation mode at 514.5 nm. The power focused on the samples was always less than 600 mW. The scattered Raman photons were detected using a thermoelectrically cooled Hamamatsu model 943XX photomultiplier that, through a photon counting chain and an acquisition board system, is computer-controlled by the ISA Jobin-Yvon SpectraMax package. The same software allows for automatic handling of the experiments, i.e., acquisition of rough data and its manipulation. The spectra were recorded with vertical−vertical (VV) and horizontal−vertical (HV) polarization scattering geometries by opportune setting up of a Melles-Griot polarization rotator placed before the sample. Accurate focusing was obtained via micromovements of XYZ microtranslators on which all of the entrance and collecting lens were mounted.

The temperature was controlled by circulating water from a Haake F6 ultra-thermostat permitting a precise temperature setting of ±0.1 °C. An electronic thermometer mounted in the measure cell controlled the exact temperature values of the samples.

3. Methodologies Used for Obtaining and Analyzing the Experimental Results

One analytical procedure we adopted consisted of comparing the spectra of glucose aqueous solutions with those of pure water in the OH-stretching region of IR and Raman signals. This method is now well-established[21,37] for following the water structure modifications operated by different solutes. In fact, the OH-stretching total distribution can be assigned to oscillators belonging to the mixture of different H-bonded structures.[38−40]

Both the IR and VV polarized Raman spectra of pure water were fitted to reproduce the OH-stretching (ν_{OH}) contour by means of three components. Different approaches were adopted to reproduce experimental profiles; in the present work we decided to employ the minimum number of parameters in order to achieve a better comparison of different samples. Moreover, the three subbands can be clearly recognized in the total envelope of IR and Raman OH-stretching signals. The fitting procedure was performed by fixing the number and the functional shape of the relevant components and allowing the remaining parameters, i.e., frequencies, intensities, and bandwidths, to vary without constraints. In particular, the deconvolution procedure of Marinov and co-workers[41] was used for the analysis of Raman spectra. In accordance with this procedure, the OH stretching band was fitted with three contributions: a mixed 50% Gaussian−50% Lorentzian shape for the low-frequency component and two Gaussian shapes for components at higher frequencies. The method of Freda et al.[40] was applied to reproduce IR measurements by means of Gaussian profiles. In both cases, the experimental profiles are very nicely reproduced through the use of three curves centered at 3215, 3425, and 3615 cm^{-1} in the VV Raman spectrum and at 3300, 3470 and 3610 cm^{-1} in the IR spectrum of water at 25 °C (Figure 1). The assignment of these three components was determined on the basis of literature data,[30,38,40] i.e., attributing the lower frequency component (G_1) to ordered tetrahedral H-bonded structures (open structures), the medium-frequency one (G_2) to distorted H-bonded structures (closed structures), and the higher frequency one (G_3) to water molecules having free hydroxyls. This assignment is suggested by the temperature, pressure, and polarization behavior of the three subbands. Moreover, the properties of G_1 and G_2 components are in good agreement with those of the low- and high-density forms of liquid water as probed by molecular dynamics simulations.[42] It has been shown[38] that owing to its action on the order−disorder structural equilibrium of the H-bonding network of bulk water, temperature influences the relative intensities of these distributions by evidencing isosbestic points. The solutes increase the intensity of the low-frequency component when they have structuring effects on bulk water (hydrophobic hydration) and lower the intensity of this component when they exert, as the electrolytes, destructuring effects.

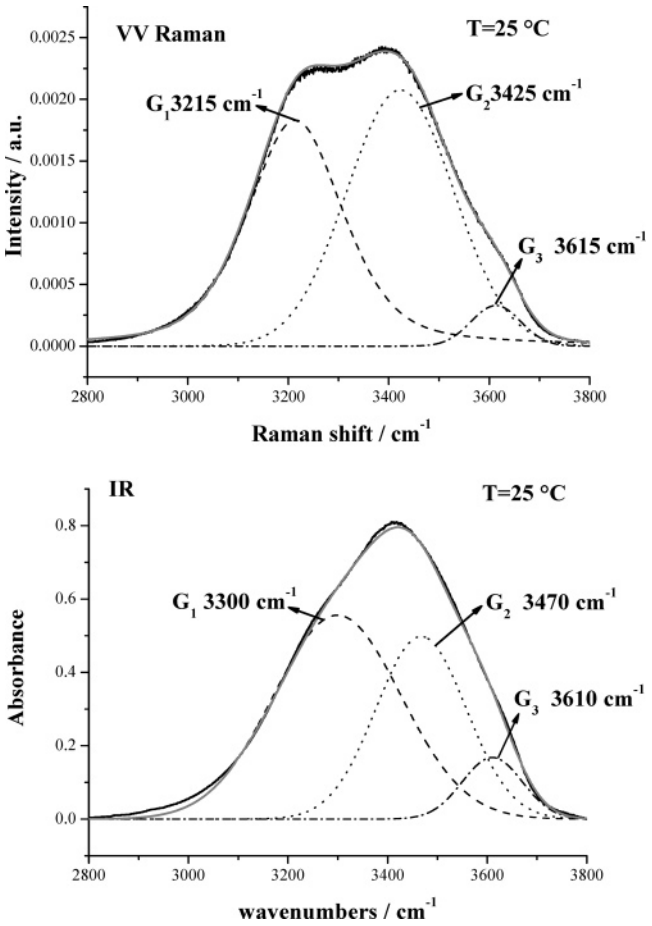

Figure 1. Room-temperature VV polarized Raman (upper part) and FTIR (lower) spectra of water, together with the fitting results: total curve (gray line) and $G_1-G_2-G_3$ components.

It is important to note that the position of the highest frequency component of IR and polarized Raman profile is very similar. On the contrary, the G_1 and G_2 bands are red-shifted in Raman with respect to IR absorption. This is due to the quite different sensitivity of the two techniques to the distribution of H-bonded ν_{OH} oscillators. In particular, the polarized Raman spectrum demonstrates greater sensitivity in detecting the ordered region of liquid water; this fact shifts the maximum of the relevant distribution to lower frequencies.

In the light of this observation, we adopted the Green, Lacey, and Sheats (GLS) procedure[43−45] to isolate the contribution associated with the icelike region of both pure water and solution Raman spectra. The results of this procedure were able to give us an idea of structuring or destructuring effects exerted by this solute.

The method is based on the assumption that the HV Raman profile of liquid water does not have the contribution of the in-phase stretching vibration, which is strongly polarized. In fact, on the basis of the mixture model of liquid water, the low-frequency component of the Raman spectrum is the collective stretching mode of the in-phase tetrahedrically H-bonded water pentamers, extended in the three dimensions as in the ice crystals. The intensity of such a collective band (I_C) can be considered a measure of structural order in liquid water and is obtained by subtracting the HV intensity, after dividing it by the maximum value of the depolarization ratio in the 3100−3800 cm^{-1} range (I_{HV}/ρ_{O-H}) from the VV intensity (I_{VV}), i.e.:

$$I_C = I_{VV} - (I_{HV}/\rho_{O-H}) \tag{1}$$

In perfect agreement with literature ρ_{O-H} data, we used a measured value of 0.23.

To apply this procedure, we defined a $C_w(T)$ quantity, which measures, at any given temperature, the ratio between I_C and the polarized spectrum intensity I_{VV} measured at the same temperature, i.e.,

$$C_w(T) = I_C(T)/I_{VV}(T) \tag{2}$$

Thus, $C_w(T)$ gives a measure of the relative amount of OH groups involved in the tetrahedral HB network in pure water at temperature T.

For the glucose solutions, we defined an analogous quantity that is a function of both temperature and solute mole fraction:

$$C_G(x,T) = I_C(x,T)/I_{VV}(x,T) \tag{3}$$

Defined in this way, $C_G(x,T)$ measures the amount of collective band contribution for each glucose mole fraction and temperature. The effects induced by the sugar can be further quantified as follows. The probability (P_d) that an OH group is excluded from the tetrahedral network due to an unfavorable distance or orientation induced by the solute is[46]

$$P_d = [C_w(T) - C_G(x,T)]/C_w(T) \tag{4}$$

and the number of H-bond defective sites existing in the network per molecule of solute (N) can be calculated from the probability P_d as

$$N = (P_d/f_x)(C_w(T)/C_{ice}) \tag{5}$$

where f_x is the number of solute molecules per OH oscillator and C_{ice} is the intensity of the in-phase collective spectrum for the perfectly H-bonded ice. The $(C_w(T)/C_{ice})$ term takes into account the number of defects in water at temperature T with respect to the situation of maximum order of crystalline ice. As a result, the N value estimates only the effects due to the solute.[47] The N value reported for different molecules can be used to compare the effects linked to different solutes in aqueous solutions.

A different probe for the study of perturbations on water structure induced by glucose is the mid-frequency HÔH bending mode. The acquisition of FTIR spectra in the entire middle-IR region allowed comparing the spectral properties of the two different modes (stretching and bending) recorded simultaneously. Information on the properties of solutions is extrapolated from the temperature and concentration behavior of these different vibrations in the spectra of our samples.

4. Results

The IR and Raman spectra of pure water were recorded in the 5−80 °C temperature range. These spectra were compared with those of glucose solutions with $0.029 \le x_G \le 0.120$ at the same temperatures (x_G = glucose mole fraction).

In Figure 2a, the OH-stretching region of the VV Raman spectra of water and two glucose solutions are shown at 25 °C. It can be observed that the increase in sugar concentration produces an evident decrease in intensity for the high wavenumbers shoulder. Less remarkable intensity variations are observed in the regions corresponding to lower frequency components of VV polarized Raman spectrum.

The same comparative analysis on the FTIR spectra of water and glucose solutions at 25 °C is shown in Figure 2b. In this case, together with the reduction of solutions absorbance around

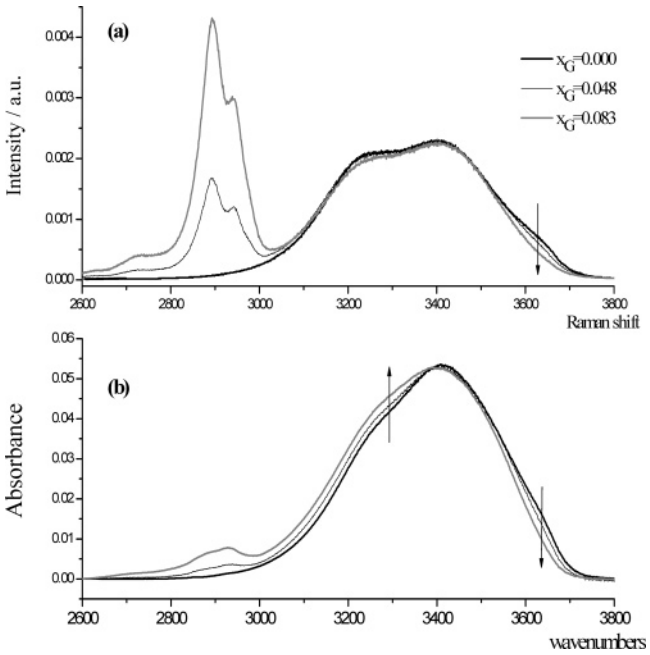

Figure 2. VV Raman (a) and FTIR (b) spectra of water and solutions at room temperature.

3600 cm^{-1}, one can note weak intensity increments in the low wavenumbers side (at about 3300 cm^{-1}) of the OH-stretching spectrum. These effects are enhanced by increasing the glucose content in solutions.

In Figure 3a, the comparison between the depolarized Raman (HV) spectra of pure water and two glucose solutions is shown. These spectra look very similar to the FTIR spectra of Figure 2b. They once again show intensity reduction at higher frequencies and intensity increases at lower frequencies of the depolarized ν_{OH} distribution. In Figure 3b, the wavenumber dependence of the depolarization ratio (ρ) for water and two glucose solutions is compared. The ρ values, having an *x*-dependence in the 3100−3500 cm^{-1} region, will be used to evaluate structural effects as described below.

(a) Curve-Fitting Analysis. Owing to the solute's limited effect on the spectral shape of the OH-stretching distributions, we applied the VV Raman spectra of glucose solutions to the same fitting procedure described for water and extracted the relevant integrated intensities for the three components G_1, G_2, and G_3. The agreement between calculated and measured profiles was still very good ($R \geq 0.96$) and showed that sensitive intensity variations are limited to the G_3 band, in agreement with the above description of experimental data.

In Figure 4 the ratio I_3/I_{TOT} ($I_{TOT} = I_1 + I_2 + I_3$) calculated from VV profiles is reported as a function of the glucose mole fraction at room temperature. I_1, I_2, I_3 are the integrated intensity of G_1,G_2, and G_3 bands, respectively. It clearly emerges that this ratio is steeply descendent with the increase in glucose concentrations, indicating that glucose captures the free hydroxyls of water molecules.

The 3100−3400 cm^{-1} range of FTIR and HV Raman profiles presents an x_G dependence more evident than in polarized Raman profiles. Thus, the comparison between Figures 2a,b and 3a could suggest that the VV Raman measurements have a different sensitivity to the properties of water with respect to IR and HV Raman spectra. The similarities between IR and depolarized scattering profiles have been claimed in the literature.[43]

To further inspect the spectral properties of solutions, we compared the IR spectra of the $x_G = 0.083$ solution (S), the crystalline solid α-D-glucose (CS), and a hydrated form of amorphous solid glucose (AS). Spectral features are shown in Figure 5.

The OH-stretching intensity of the crystalline sugar is much lower than the solution counterpart, so that we can assume a negligible solute contribution to the ν_{OH} solution spectra. This fact justifies once again the possibility of analyzing the spectra of solutions in the ν_{OH} region as essentially due to water contribution. Moreover, the 3100−3800 cm^{-1} CS absorbance is largely due to the HB glucose−glucose interactions that are not present in solution.

In contrast, the ν_{OH} distribution for the AS has a much higher intensity than for CS. This intensity is most probably due to the presence of the water surrounding the amorphous solid and to its HB interaction with the carbohydrate. This AS profile is thus indicative of the spectral properties of hydration water. For this sample, the water bending absorption around 1640 cm^{-1} is also clearly visible in the FTIR spectrum.

The inset of Figure 5 shows that the ν_{OH} distribution for the hydrated amorphous sample is red-shifted relative to the bulk water at the same temperature, with a center at around 3380 cm^{-1}. This observation suggests that the strength of water−sugar H-bonding interactions is appreciable, being intermediate to those of G_1 and G_2 components of neat water. At higher wavenumbers, the contribution from free OH oscillators seems to be completely lacking, suggesting that water and glucose OH groups are all interacting in this system.

We believe that this datum is helpful in explaining the intensity increase at low wavenumbers in the IR and HV Raman spectra of solutions, as reported in Figures 2b and 3a, respectively. If we assume that the hydration water in solution has the same characteristics of the hydration water of AS sample, we can attribute the red-shift of solution ν_{OH} distributions to this species; in fact, it does not contribute to the intensity at higher wavenumbers. As a consequence, when applying the three-band deconvolution of IR solution spectra, the agreement between fitting and experiment is still valid, but the G_1 and G_2 subbands will reflect contributions coming from the hydration water also. The presence of an additional contribution is confirmed by the analysis of depolarization ratio curves as shown in Figure 3b. The 3100−3500 cm^{-1} ρ values increase on increasing x_G, and this cannot be due to the different equilibrium among structures of bulk water. It could instead be connected to the additional presence of a lower symmetry arrangement: the one resulting from the hydration water. On the contrary, the variation of the high wavenumbers component is due only to bulk water.

It is important to note how much the temperature can influence the effects induced by the glucose. In principle, the amount of free OH groups in water is expected to increase with temperature as an effect of the H-bonds breaking, so that the increase in temperature and in glucose concentration should be conflicting factors. We have assigned to non H-bonded ν_{OH} oscillators (NHB) the G_3 component around 3600 cm^{-1} and to H-bonded species (HB) both the G_1 and G_2 subbands. The variation of free hydroxyls with respect to HB ones can be followed through the trend of the NHB/HB ratio. Figure 6 shows the temperature behavior of this quantity for pure water and solutions as calculated from IR spectra. We remark that this ratio in the solutions reflects the presence of water−glucose species together with those of bulk water. Therefore, the fitting procedure applied to IR OH-stretching absorptions can be used to make an estimation of the average strength of interaction in solution. In fact, according to the two-state model,[31,33,35] the

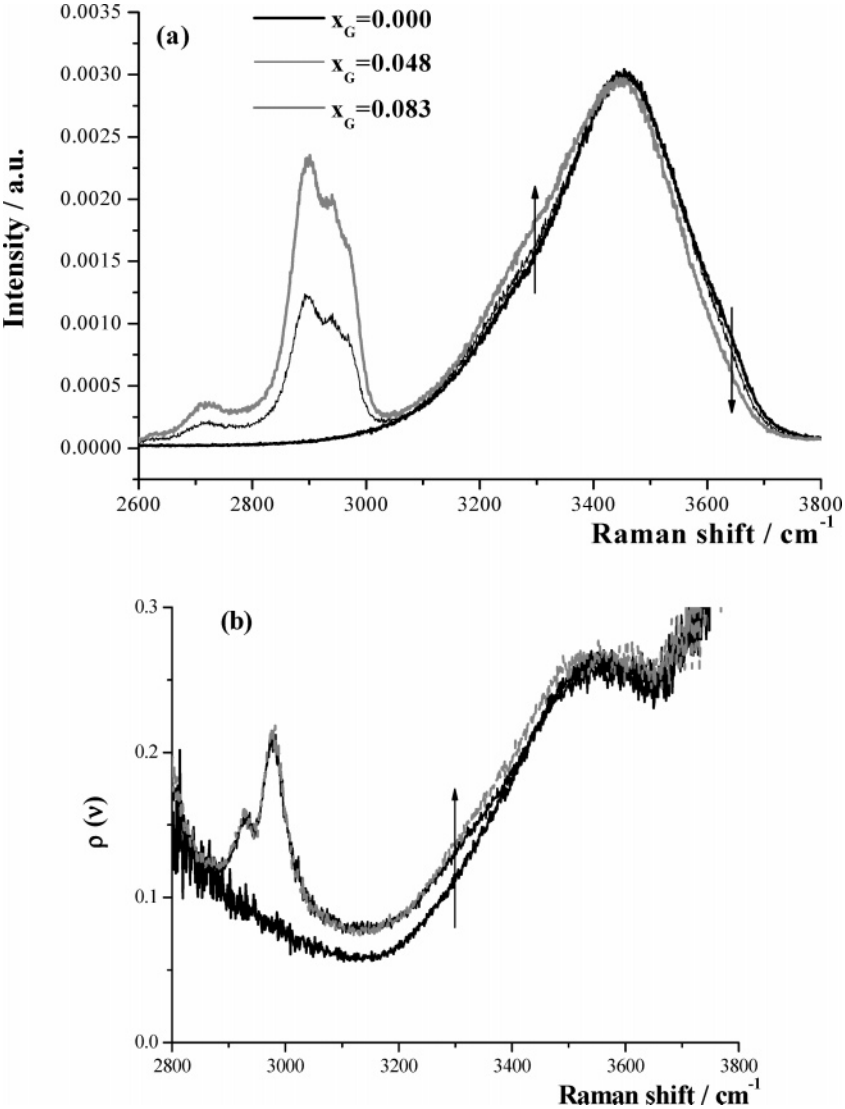

Figure 3. HV Raman spectra (a) and depolarization ratio values (b) of water and glucose solutions at room temperature.

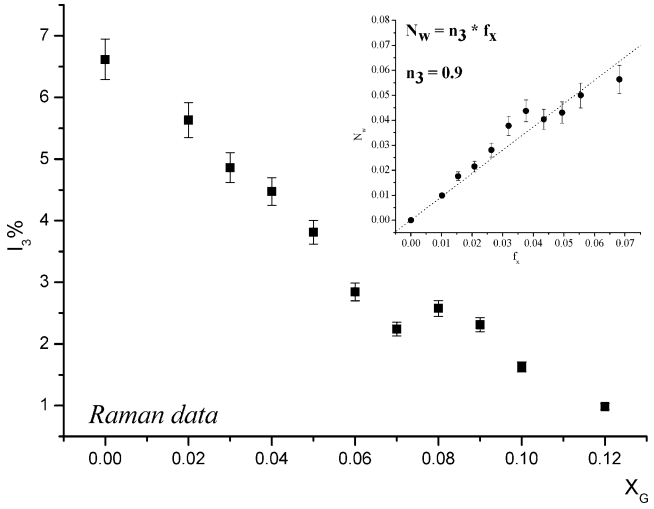

Figure 4. Concentration dependence of the I_3 integrated intensity as calculated from fitting procedure of VV Raman spectra at room temperature. The inset of the figure shows the f_x dependence of the free oscillators fraction (N_w) captured by glucose.

average (water−water and water−glucose) H-bonding enthalpy (ΔH_{HB}) can be evaluated through the van't Hoff plot of the NHB/HB ratio. These values are reported in Table 1. The ΔH_{HB} of solutions are compared with that of pure water obtained through the same procedure: reduced ΔH_{HB} values are observed on increasing glucose content. This fact could suggest an overall destructuring effect induced by glucose on liquid H_2O.

(b) GLS Procedure. We now focus on the properties of the low wavenumbers ν_{OH} oscillators. The procedure described in the methodology section (GLS procedure[43−45]) is very useful for obtaining information on the tetrahedrally ordered structure of bulk water and on its modifications effected by the solutes. The C_G quantity described in the previous section is plotted as a function of x_G at room temperature in Figure 7, where the C_w value is also given.

We can clearly observe a decrease in C_G upon increasing the glucose content. This means that the glucose addition reduces the contribution of in-phase collective motion to the total ν_{OH} distribution, i.e., the extension of icelike structures of bulk water. Even though the action is not as large as those reported for trehalose,[21] some destructuring effects on the ordered H-bonded network of water are detectable on the basis of these results.

(c) The HÔH Bending Mode of Liquid Water. Usually, the structural properties of water in solutions are efficiently probed by vibrational spectroscopies following the characteristics of the OH-stretching profiles. Nevertheless, some useful indications can also come from the analysis of the HÔH bending motion. The IR spectrum of liquid water shows a 1640 cm^{-1}

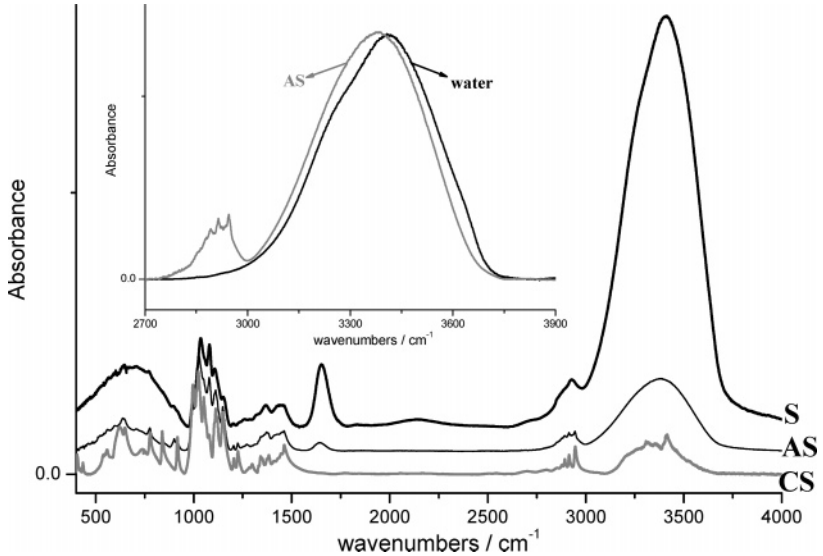

Figure 5. FTIR spectra of $x_G = 0.083$ solution (S), amorphous solid (AS), and α-D-glucose crystalline solid (CS) at room temperature. The different spectra are normalized on the intensity of the 1000−1200 cm^{-1} glucose absorption. The OH-stretching region of water (solid line) and AS (dotted line) FTIR spectra is reported in the figure inset.

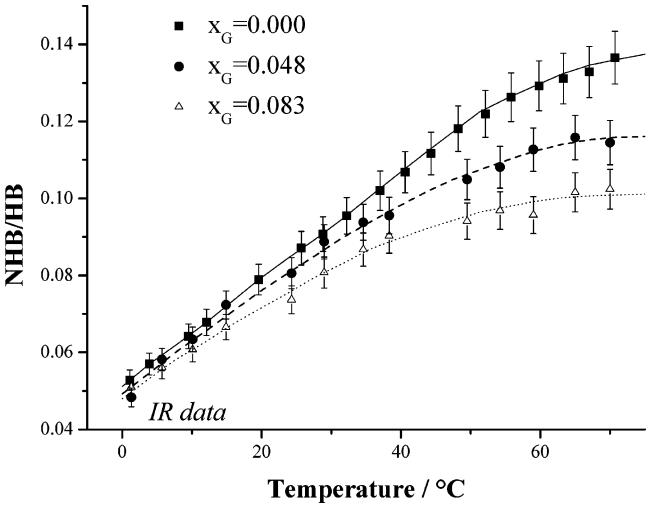

Figure 6. Temperature dependence of NHB/HB ratio evaluated by curve-fitting analysis of FTIR spectra of water and two glucose solutions.

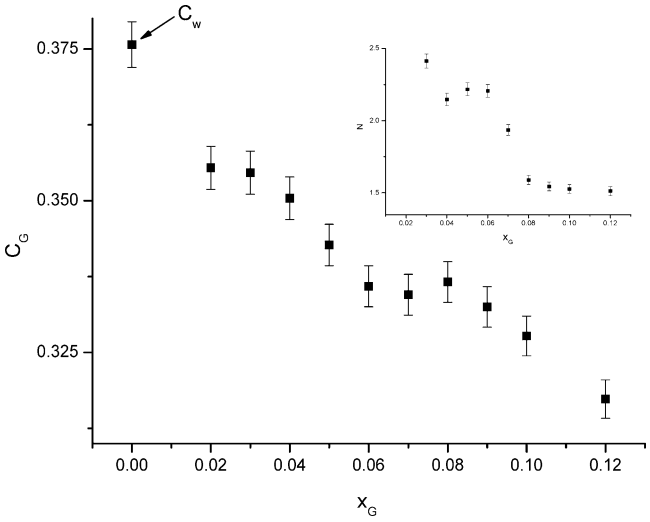

Figure 7. x_G dependence of C_G and N (see inset) parameters evaluated by the GLS stripping procedure.

TABLE 1: H-Bonding Enthalpy for Glucose Aqueous Solutions

	$x_G = 0.000$	$x_G = 0.048$	$x_G = 0.083$
ΔH_{HB}/kcal mol^{-1}	2.54 ± 0.10	2.20 ± 0.20	1.80 ± 0.10

band associated with this mode. The behavior of this absorption is largely reported in the literature[48−50] as giving a red shift and a sharpening on the temperature increase.

In Figure 8 the position and width of the 1640 cm^{-1} band is reported as a function of temperature for neat water and for two glucose solutions. In this case we are certain that no interference can come from solute absorptions; as a consequence, the differences produced in this spectral region can only be ascribed to a change in water structure properties.

As we can see, both band parameters are sensitive to the addition of glucose. If we look at the effects on band position and bandwidth operated by glucose, we can observe that this sugar influences the thermal behavior of both band parameters. This is shown by the different slopes of pure water and solutions in the relevant plots. Given the red shift of the band position we might think that the addition of glucose has an effect similar to the decrease in temperature, but the width of the band shows an opposite trend.

5. Discussion

Experimental data show that the more visible effect of the glucose is a reduction in the free water hydroxyls. Consequently, we may suppose that the hydration shell of glucose includes a partial contribution originating from the free OH groups of water. The hydrogen bonds of glucose−water hydrates have been investigated by DFT calculations of infrared spectra of glucose aqueous solutions.[51] These authors postulated that the number of water molecules H-bonded to glucose ranges from four to nine. The computed infrared spectra were most in agreement with the experimental counterpart when eight or nine water molecules were explicitly considered around one glucose molecule.

The amount of free OHs in bulk water at room temperature is too low to suppose that glucose can complete its first hydration layer utilizing only these kinds of hydroxyls. A quantitative estimate of this contribution can be achieved through our spectroscopic data. In fact, we can use the value of the integrated

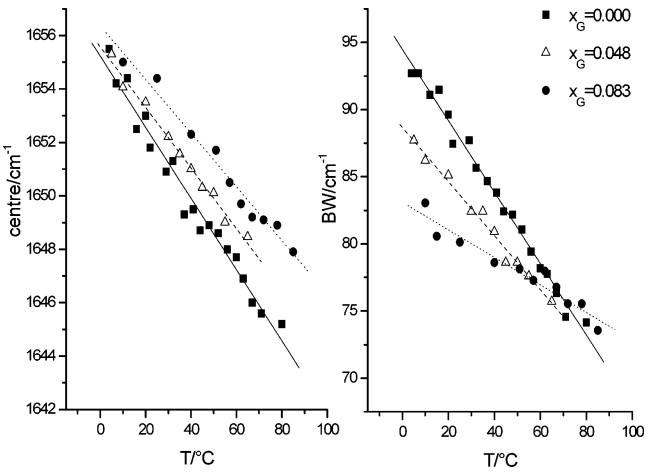

Figure 8. Temperature dependence of the position (center) and bandwidth (BW) of H_2O bending band measured in the FTIR spectra of water and two glucose solutions.

intensity I_3 to measure free hydroxyl concentrations. Moreover, we can assume that the diminishment of I_3 in solution with respect to pure water is exactly proportional to the fraction of oscillators (N_w) captured by glucose molecules. In the inset of Figure 4 this number is reported as a function of f_x, with f_x being the quantity defined before. The linear dependence of N_w vs f_x gives a slope of 0.9, and this suggests that about one hydroxyl per solute molecule is captured. The reduction of free hydroxyls contributes to red-shifting the ν_{OH} distribution of (bulk + hydration) water, as shown in Figure 2b. This indicates the presence of a higher number of H-bonds in solution with respect to neat water. This could be related to the increase of viscosity with increasing sugar content.[52]

When we apply the GLS procedure to our solutions, we may observe that glucose produces small but quantitatively appreciable intensity variations that are enhanced at the higher sugar concentrations. These variations consist of small intensity decrements indicated by the I_c or C_G values. As a consequence, we can assume that glucose has a small destructuring effect on the bulk structure of water.

Thus, besides the effects described above, the glucose−water interaction extending beyond the first hydration shell individuates short-range modifications in the ordered "open" structure shown by the reduction of the collective mode intensity. The reduction of this mode intensity is a measure of the number of defects N (see eq 5) introduced in the tetrahedral network of H_2O per glucose molecule;[47] the results are shown in the inset of Figure 7. N can be associated with the number of H-bonds broken in the tetrahedral network of bulk water due to the glucose−water interactions in the hydration shell. The dependence of this parameter on x_G suggests that at low concentration the average number of defects per sugar molecule is 2.2 ca. The N value is weakly concentration-dependent, becoming ca. 1.6 when $x_G \geq 0.08$. This could be due to the overlapping of hydration shells among solute molecules and to the establishment of glucose−glucose H-bonds; this latter effect reduces the probability of solute−solvent interactions. The concentration dependence of this parameter is in agreement with the results of molecular dynamics simulations.[27] These N values are very close to those of dextran solutions obtained in the same concentration range.[46]

Generally speaking, the OH-stretching distribution of solutions provides important information on the properties of bulk and hydration water. Within this distribution we can identify two types of oscillators characteristic of bulk water: free hydroxyl groups resonating at higher wavenumbers and tetrahedrally ordered HB oscillators resonating at lower wavenumbers. Both types of OH groups are captured by glucose functionalities to constitute the hydration shell. Of course, water molecules participating in the shell do not derive from these two different kinds of structures alone; most of the solvating water molecules are subtracted from disordered HB assemblies of the bulk. Unfortunately, the vibrational spectroscopies have the limit of not being able to distinguish the disordered oscillators of hydration or bulk water. On the other hand, this fact could suggest that the glucose−water interaction is as strong as the water−water interaction of closed structures.

In the light of the measured ΔH_{HB} values, we can say that the reduction of ordered, icelike structures causes a considerable decrease in the average interaction strength. In fact, the low-frequency oscillators are the most temperature-dependent (stronger H-bonding interaction), and although the addition of carbohydrates induces an increase in the number of H-bonds per molecule, the overall HB strength is reduced. This result is very important, as it supports the theories that link the conservative action of solutes to their effects on the tetrahedral structure of water.[18−21]

The analysis of the bending $\delta_{H\hat{O}H}$ mode provides further support to the description above. In fact, if we refer to the data of Figure 8 we can say that the effect of adding glucose on band position recalls that of a decrease in temperature, while the effect on the bandwidth is similar to an increase in temperature.

To understand the first of these two effects, we must consider that in the bending mode also, as in ν_{OH} distribution, it is possible to recognize the two NHB and HB species. In that case, the NHB component is found at lower wavenumbers while the HB one resonates at higher wavenumbers. Most of this signal intensity is due to those water molecules less involved in the H-bonding network.[40] In this respect, the analysis of this signal constitutes a sensitive probe for the free OH groups that contribute little to the total OH-stretching distribution.

The trend reported in Figure 8 suggests that the NHB molecules diminish with increasing glucose content in solution; in fact, an increase in NHB species would have shifted the band to the red like an increase in temperature.

The behavior of the bandwidth (BW) also is indicative of water−glucose interactions. In fact, it has been reported that the width of $\delta_{H\hat{O}H}$ as a function of temperature in bulk water essentially depends on an inhomogeneous broadening.[39,53] This means that at low temperatures the bending motion probes an inhomogeneous distribution of oscillators (large BW). On the contrary, an increase in temperature removes this inhomogeneity, sharpening the band profile. This homogeneous or inhomogeneous distribution of oscillators can be related to the HB capability of the liquid system. In fact, at low temperature both ordered and disordered HB structures are probable together with NHB species, while at higher temperatures, $\delta_{H\hat{O}H}$ absorption is mainly caused by the NHB class of oscillators.

We believe that the x_G dependence shown in Figure 8 can have a similar origin. At low temperatures, the bending mode is positioned toward the HB component, but the wide $\delta_{H\hat{O}H}$ distribution is reduced after glucose addition due to the reduction of both highly ordered (icelike) and highly disordered (free OHs) species; as a result, the bending mode BW has lower values in solutions. On the contrary, at high temperature the bending motion essentially probes the NHB oscillators both in bulk water and in solutions, so that no concentration dependence is observed. In the case of $\delta_{H\hat{O}H}$ absorption as well, the temperature

dependence of both position and bandwidth is greater in neat water than in the solutions.

These results strongly support our IR and Raman analysis of the OH-stretching distribution described above.

6. Conclusions

The vibrational analysis of the OH-stretching and HÔH bending distributions in the infrared and Raman spectra of a series of glucose aqueous solutions allows highlighting some interesting aspects on glucose−water interactions. It has been observed that when dissolving glucose in water, an evident solute action is the removal of free water hydroxyls from the bulk liquid. This may be easily deduced considering the consistent intensity reduction of the shoulder around 3600−3650 cm^{-1} in the Raman VV and HV profiles and in the infrared spectra. The reduced amount of free OH groups in solution (one hydroxyl *per* glucose molecule) leads to an increase in H-bonds in the liquid that also explains the observed increase in viscosity.

Specific water−glucose H-bonds are established and are revealed by the small absorbance increase at around 3300 cm^{-1} in the IR spectra and by the scattering cross section increase in the same region of the depolarized Raman spectra. At these wavenumbers, no intensity variations can be detected in the VV Raman profiles. This is because the strong intensity of the collective in-phase OH-stretching mode has an opposite concentration dependence. To solve this problem one can use different spectroscopic techniques: this is fundamental in achieving a complete description of the phenomenon.

Even though the effect of solutes on tetrahedral arrangement of H_2O has been the object of much study, our results provide new insights. In fact, the glucose constitutes a somewhat controversial case in the literature,[27,54−57] owing to the lack of ample experimental data. In this respect our study gives a lot of information, for it probes these effects in a wide temperature and concentration range. As regards analysis of the collective mode, the use of the GLS stripping procedure has shown a small but appreciable destructuring effect operated by glucose on the long-range icelike ordered structure of liquid water. This effect is confirmed by MD simulation studies on glucose−water mixtures in almost the same concentration range.[22,48] Relative to the results obtained through the use of the GLS procedure, our position is a bit different from those of previous authors. Maeda and co-workers, for example,[40] interpret the reduction of icelike structures as indicative of a decrease in H-bonds in solutions. We instead believe that the water−water interaction for molecules participating in these structures is substituted by water−glucose interaction in the hydration shell. Thus the destructuring effect does not lead to an effective reduction in the H-bonding network; as shown above, the number of H-bonds is higher in solution than in pure water. This could be very important for the comprehension of bioprotective properties of sugars. In fact, we believe that the reduced temperature dependence observed in our spectra can be related to the ability of glucose to preserve the structure of water under temperature stress even in the presence of biomolecules. Moreover, the decrease in free OH groups upon addition of glucose (or carbohydrates in general) reduces the possibility of HB interactions between macromolecules (protein or enzyme) and water. In fact, the free hydroxyls are the most reactive sites of water's structure; a reduction in these sites could probably justify the inhibition of the conformational rearrangement of biomolecules that is leading to the unfolding process.

The present structural effects on bulk water are weak, considering that our measurements extend from much diluted to moderately high glucose concentrations; this result confirms recent MD simulation findings on glucose aqueous solutions.[58]

Moreover, our results are in perfect agreement with those interpretations correlating effectiveness in protecting biomolecules with the destructuring effect of carbohydrates.[18−26] In fact, glucose solutions have less efficient protective and conservation properties in comparison with those of its dimers trehalose and sucrose, which realize a stronger reduction in the icelike structure of water.

Acknowledgment. The authors appreciate the financial support given to this research by Ministero dell'Istruzione, Università e Ricerca (MIUR, Roma), under the COFIN 2003 project. They are also grateful to Prof. Giulio Paliani for useful discussions, and to Prof. Aldo Santucci for his kind support in the realization of the vacuum IR cell.

References and Notes

(1) Oksanen, C. A.; Zografi, G. *Pharm. Res.* **1990**, *7*, 654.
(2) Franks, F.; Hatley, R. H. M.; Mathias, S. F. *BioPharm (Duluth, Minn.)* **1991**, *4*, 38.
(3) Cleland, J. L.; Langer, R., Ed. In *Formulation and Delivery of Proteins and Peptides;* ACS Symposium Series 567; American Chemical Society: Washington, DC, 1994.
(4) Franks, F., Hatley, R. H. M. In *Stability and Stabilization of Enzymes*; van den Tweel, W. J. J., Harder, A., Buitelaar, R. M., Eds.; Elsevier Science: New York, 1993.
(5) Roberts, C. J.; Debenedetti, P. G. *AIChE J.* **2002**, *48*, 1140.
(6) Mrevlishvili, G. M. *Thermochim. Acta* **1998**, *308*, 49.
(7) Almond, A.; Duus, J.Ø. *J. Biomol. NMR* **2001**, *20*, 351.
(8) Almond, A.; Sheehan, J. K. *Glycobiology* **2003**, *13*, 255.
(9) Almond, A. *Carbohydr. Res.* **2005**, *340*, 907.
(10) Jockusch, R. A.; Talbot, F. O.; Asano, N.; Fleet, G. W.; Simons, J. P. *PCCP* **2004**, *6*, 5283.
(11) Çarçabal, P.; Jockusch, R. A.; Hünig, I.; Snoek, L. C.; Kroemer, R. T.; Davis B. G.; Gamblin, D. P.; Compagnon, I.; Oomens, J.; Simons, J. P. *J. Am. Chem. Soc.* **2005**, *127*, 11414.
(12) Crowe, J. H.; Carpenter, J. F.; Crowe, L. M. *Annu. Rev. Physiol.* **1998**, *70*, 73.
(13) Donnamaria, M. C.; Howard, E. I.; Grigera, J. R. *J. Chem. Soc., Faraday Trans.* **1994**, *90*, 2731.
(14) Caffarena, E. R.; Grigera, J. R., *J. Chem. Soc., Faraday Trans.* **1996**, *92*, 2285.
(15) Howard, E. Y.; Grigera, J. R. *Carbohydr. Res.* **1996**, *282*, 25.
(16) Caffarena, E. R.; Grigera, J. R. *Carbohydr. Res.* **1997**, *300*, 51.
(17) Caffarena E. R.; Grigera J. R. *Carbohydr. Res.* **1999**, *315*, 63.
(18) Magazù, S.; Maisano, G.; Migliardo, P.; Middendorf, H. D.; Villari V. *J. Chem. Phys.* **1999**, *109*, 1170.
(19) Magazù, S.; Migliardo, P.; Musolino, A. M.; Sciortino, M. T. *J. Phys. Chem. B* **1997**, *101*, 2348.
(20) Magazù, S.; Maisano, G.; Migliardo, P.; Tettamanti, E.; Villari, V. *Mol. Phys.* **1999**, *381*, 96.
(21) (a) Branca, C.; Magazù, S.; Maisano, G.; Migliardo, P. *J. Chem. Phys.* **1999**, *111*, 281. (b) Branca, C.; Magazù, S.; Maisano, G.; Migliardo, P. *J. Phys. Chem. B* **1999**, *103*, 1347.
(22) Branca, C.; Magazù, S.; Maisano, G.; Bennington, S. M.; Fak, B. *J. Phys. Chem. B* **2003**, *107*, 1444.
(23) Magazù, S.; Villari, V.; Migliardo, P.; Maisano, G.; Telling, M. T. F. *J. Chem. Phys.* **2001**, *115*, 1851.
(24) Faraone, A.; Magazù, S.; Lechner, R. E.; Longeville, S.; Maisano, G.; Majolino, D.; Migliardo, P.; Wanderlingh, U. *J. Chem. Phys.* **2001**, *115*, 3281.
(25) Branca, C.; Faraone A.; Magazù, S.; Maisano, G.; Mangione, A.; Pappas, C.; Triolo, A. *Appl. Phys. A* **2002**, *74*, S461.
(26) Branca, C.; Magazù, S.; Maisano, G.; Migliardo, F. *Phys. Rev. B* **2001**, *64*, 224204.
(27) Roberts, C. J.; Debenedetti, P. G. *J. Phys. Chem. B* **1999**, *103*, 7308.
(28) Franks, F., Ed.; In *Water Science Review*; Cambridge University Press: Cambridge, 1988; Vol. 3.
(29) Green J. L.; Angell, C. A. *J. Phys. Chem.* **1989**, *93*, 2880.
(30) Robinson, G. W.; Cho, C. H.; Urquidi, J. *J. Chem. Phys.* **1999**, *111*, 698.
(31) Sassi, P.; Morresi, A.; Paolantoni, M.; Cataliotti, R. S. *J. Mol. Liq.* **2002**, *96*−*97*, 363.
(32) Raudino, A.; Sassi, P.; Morresi, A.; Cataliotti, R. S. *J. Chem. Phys.* **2002**, *117*, 4907.

(33) Sassi, P.; Paolantoni, M.; Morresi, A. *Chem. Phys. Lett.* **2002**, *357*, 293.
(34) Sassi, P.; Marcelli, A.; Paolantoni, M.; Morresi, A.; Cataliotti, R. S. *J. Phys. Chem. A* **2003**, *107*, 6243.
(35) Paolantoni, M.; Sassi, P.; Morresi, A.; Cataliotti, R. S. *Chem. Phys.* **2005**, *310*, 169.
(36) Sassi, P.; Paolantoni, M.; Cataliotti, R. S.; Palombo, F.; Morresi, A. *J. Phys. Chem. B* **2004**, *108*, 19557.
(37) Mathlouthi, M.; Hutteau, F.; Angiboust, J. F. *Food Chem.* **1996**, *56*, 215.
(38) Walrafen, G. E.; Hokmabadi, M. S.; Yang, W. H. *J. Chem. Phys.* **1986**, *85*, 6964.
(39) Raichlin, Y.; Millo, A.; Katzir, A. *Phys. Rev. Lett.* **2004**, *93*, 185703.
(40) Freda, M.; Piluso, A.; Santucci, A.; Sassi, P. *Appl. Spectrosc.* **2005**, *59*, 1155.
(41) Marinov, V. S.; Nickolov, Z. S.; Matsuura, H. *J. Phys. Chem. B* **2001**, *105*, 9953.
(42) Errington, J. R.; Debenedetti, P. G. *Nature* **2001**, *409*, 318.
(43) Green, J. L.; Lacey, A. R.; Sceats, M. G. *J. Phys. Chem.* **1986**, *90*, 3958.
(44) Green, J. L.; Lacey, A. R.; Sceats, M. G., *Chem. Phys. Lett.* **1987**, *134*, 385.
(45) Green, J. L.; Lacey, A. R.; Sceats, M. G. *J. Chem. Phys.* **1987**, *87*, 3603.
(46) Maeda, Y.; Tsukida, N.; Kitano, H.; Terada, T.; Yamanaka, J. *J. Phys. Chem.* **1993**, *97*, 13903.
(47) Kitano H.; Imai, M.; Mori, T.; Gemme-Ide, M.; Yokoyama, Y.; Ishihara, K.; *Langmuir* **2003**, *19*, 10260.
(48) Maréchal, Y. *J. Chem. Phys.* **1991**, *95*, 5565.
(49) Maréchal, Y. *J. Phys. Chem.* **1993**, *97*, 2846.
(50) Libnau, F. O.; Toft, J.; Christy, A. A.; Kvalheim, O. M. *J. Am. Chem. Soc.* **1994**, *116*, 8311.
(51) Suzuki, T.; Sota, T. *J. Chem. Phys.* **2003**, *119*, 10133.
(52) Fuchs, K.; Kaatze, U. *J. Phys. Chem. B* **2001**, *105*, 2036.
(53) Maréchal Y. *J. Mol. Struct.* **1994**, *322*, 105.
(54) De Xammar Oro, J. R. *J. Biol. Phys.* **2001**, *27*, 73.
(55) Brady, J. W. *J. Am. Chem. Soc.* **1989**, *108*, 5155.
(56) Brady, J. W. *Adv. Biophys. Chem.* **1990**, *1*, 155.
(57) Lee, S. L.; Debenedetti, P. G.; Errington J. R. *J. Chem. Phys.* **2005**, *122*, 204511.
(58) Mason, P. E.; Neilson, G. W.; Enderby, J. E.; Saboungi, M.-L.; Brady, J. W. *J. Phys. Chem. B* **2005**, *109*, 13104.